1985

NASA/ASEE SUMMER FACULTY RESEARCH FELLOWSHIP PROGRAM

MARSHALL SPACE FLIGHT CENTER
THE UNIVERSITY OF ALABAMA
IN HUNTSVILLE

SOME ENERGY CONSIDERATIONS IN GAMMA RAY BURST LOCATION DETERMINATIONS BY AN ANISOTROPIC ARRAY OF DETECTORS

Prepared by:	John H. Young
Academic Rank:	Associate Professor
University:	University of Alabama at Birmingham
Department:	Physics
NASA/MSFC:	
Laboratory:	Space Science
Division:	Astrophysics
Branch:	High Energy Physics
MSFC Counterpart:	Gerald J. Fishman

Date:	August 16, 1985
Contract Number:	NGT 01-008-021 The University of Alabama in Huntsville

SOME ENERGY CONSIDERATIONS IN GAMMA RAY BURST LOCATION DETERMINATIONS BY AN ANISOTROPIC ARRAY OF DETECTORS

BY

John H. Young
Associate Professor of Physics
University of Alabama at Birmingham
Birmingham, Alabama

ABSTRACT

The anisotropic array of detectors to be used in the Burst and Transient Source Experiment (BATSE) for locating gamma ray burst sources is examined with respect to its ability to locate those sources by means of the relative responses of its eight detectors. It has been shown that the energy-dependent attenuation effects of the aluminum window covering each detector has a significant effect on source location determinations. Location formulas have been derived as a function of detector counts and gamma ray energies in the range 50 - 150 keV. Deviation formulas have also been derived and serve to indicate the location error that would be caused by ignoring the influence of the passive absorber.

ACKNOWLEDGEMENTS

I am genuinely grateful for having been given the honor and opportunity to participate in the NASA/ASEE Summer Faculty Fellowship Program. The hospitality, facilities, and exposure to the operations of the MSFC have afforded a valuable experience and appreciation of the enviable record of achievement of the Center.

My counterpart, Dr. Gerald Fishman, and his BATSE colleagues warrant special thanks for accepting my participation in a research area which was completely new to me. I hope that our collaboration will continue with mutual benefit.

LIST OF FIGURES

LIST OF TABLES

INTRODUCTION

One of the four experiment packages aboard the Gamma Ray Observatory (GRO), scheduled for release into orbit from a shuttle flight in May 1988, is the Burst and Transient Source Experiment (BATSE). Utilizing an array of eight NaI(Tℓ) detectors BATSE will, as one of its major objectives, attempt to determine the angular locations of gamma ray burst sources by means of analyzing the relative count responses of the detector array. Figure 1 depicts the GRO configuration[1]. If the planes of the detector faces, each having an area of about 2000 cm^2, were extended so as to form a closed surface, that surface would be the regular octohedron also depicted in Figure 1.

The 1.27 cm thick detector crystals will be overlaid by 2mm of aluminum. The gamma ray flux incident on the aluminum windows will be attenuated by that material and a diminished flux will consequently be incident on the detectors. The relative orientation of the detectors, dictated by the octohedral geometry, necessitates that gamma rays incident on one detector will have transversed a different thickness of aluminum than those incident on that detector's neighbors. Thus, in addition to being energy dependent due to the material's attenuation coefficient, the attenuation will be orientation dependent.

The work described here is the result of an effort to take the energy dependence of the relative detector responses to a burst into account in the angular location determination of the source. The energy-dependent attenuation effects are discussed and location formulas containing these effects are presented.

THE BATSE GEOMETRY

The BATSE detector array conforms to the geometry of a regular octohedron shown in Figure 2. The planes, corresponding to the eight detector faces, are identified by the numbering scheme indicated. The outward normals from the eight planes are given by the following, in which $\hat{i}$, $\hat{j}$, and $\hat{k}$ are unit vectors along the positive x, y, and z axes, respectively:

$$\begin{aligned} \hat{u}_1 &= \frac{1}{\sqrt{3}}(\hat{i} + \hat{j} + \hat{k}) & \hat{u}_5 &= \frac{1}{\sqrt{3}}(-\hat{i} - \hat{j} + \hat{k}) \\ \hat{u}_2 &= \frac{1}{\sqrt{3}}(\hat{i} + \hat{j} - \hat{k}) & \hat{u}_5 &= \frac{1}{\sqrt{3}}(-\hat{i} - \hat{j} - \hat{k}) \\ \hat{u}_3 &= \frac{1}{\sqrt{3}}(-\hat{i} + \hat{j} + \hat{k}) & \hat{u}_7 &= \frac{1}{\sqrt{3}}(\hat{i} - \hat{j} + \hat{k}) \\ \hat{u}_4 &= \frac{1}{\sqrt{3}}(-\hat{i} + \hat{j} - \hat{k}) & \hat{u}_8 &= \frac{1}{\sqrt{3}}(\hat{i} - \hat{j} - \hat{k}) \end{aligned} \tag{1}$$

The following relationships between these normals are worthy of note and will be used later:

$$\begin{gathered} \hat{u}_5 = -\hat{u}_2,\ \hat{u}_6 = -\hat{u}_1,\ \hat{u}_7 = -\hat{u}_4,\ \hat{u}_8 = -\hat{u}_3, \\ \hat{u}_4 = \hat{u}_3 + \hat{u}_2 - \hat{u}_1 . \end{gathered} \tag{2}$$

If the octohedron is imagined to be centered at the origin of a large sphere of radius R (Figure 3) from whose surface a burst originates with angular coordinates θ and ϕ, the detected

portion of the burst flux will be that which propagates along the direction $-\vec{R}/R$. Let $\vec{I}$ represent the flux density (photons per unit area) in this direction, with magnitude I_o; it can be simply represented as

$$\vec{I} = I_o(-\frac{\vec{R}}{R}) = -I_o(\sin\theta\cos\phi\hat{i}+\sin\theta\sin\phi\,\hat{j}+\cos\theta\hat{k}) \quad . \qquad (3)$$

BATSE data of interest here are derived from the incidence of $\vec{I}$ onto any combination of the eight planes of the octohedron. The number of photons passing through the i-th plane whose area is A will be

$$N_i = \hat{I}\cdot(-\hat{u}_i A) = I_o A\cos\alpha_i \quad , \qquad (4)$$

where α_i is the angle between the burst direction and $-\hat{u}_i$.

DETECTOR RESPONSE

Only under ideal, and thus rarely attainable, conditions would a detector whose outward normal is $\hat{u}_i$ actually record the number of photons given by Eqn. (4). That expression must be multiplied by the detector efficiency, resulting in a decrease from Eqn. (4). The efficiency is an energy-dependent factor which accounts for attenuation losses in the passive absorber covering the detector crystal as well as the probability that a photon will interact with the crystal upon entering it. If t and D represent, respectively, the window and crystal thicknesses, the efficiency for the case of normal incidence is given by [2]

$$\eta(E) = e^{-\mu_A(E)t}\left(1 - e^{-\mu_N(E)D}\right), \qquad (5)$$

where $\mu_A(E)$ and $\mu_N(E)$ are the energy-dependent attenuation coefficients of the aluminum and sodium iodide. If, however, a photon were to enter the system at some angle α relative to the system axis, it would transverse a thickness $t/\cos\alpha$ of absorber before getting into the crystal. Further, propagation at that angle gives the photon an increased effective thickness of crystal with which to interact and thus be recorded. The latter effect amounts to replacing D by $D/\cos\alpha$ in Eqn. (5). The detector efficiency will be used here in the form

$$\eta(E) = e^{-\mu_A(E)t/\cos\alpha}\left(1 - e^{-\mu_N(E)D/\cos\alpha}\right). \qquad (6)$$

The number of photons, N_i, recorded by the i-th detector will then be given by the product of Eqns. (4) and (6); that is

$$N_i(E,\theta,\phi) = I_o A \cos\alpha_i e^{-\mu_A(E)t/\cos\alpha_i}\left(1 - e^{-\mu_N(E)D/\cos\alpha_i}\right). \qquad (7)$$

The energy dependence of the N_i considered here will be the result of the attenuation coefficients' dependence on photon energy. The relationship of N_i to the angular location of the burst is dictated by the functional relationship between α_i and (θ,ϕ); these relationships are easily determined from Eqns. (1), (3), and (4). The objective of the present work is to develop the means of determining θ and ϕ in terms of the recorded

detector counts, N_i. It is apparent from Eqn. (7) that the computation of the angular coordinates of the burst will give results dependent on photon energy. The following discussion will, in particular, be focussed on the sort of corrections required in location determinations mandated by the inclusion of energy considerations above 50 keV.

The exponential function $e^{-\mu t/\cos\alpha}$ has maximum value $(0<\alpha<90^0)e^{-\mu t}$, corresponding to normal incidence. Table 1 lists the attenuation coefficient values for aluminum[3] over the energy range of interest (50 - 200 keV) and compares the value of the exponential $e^{-\mu t}$ for t = 0.2 cm with its linear approximation, $1 - \mu t$. The largest discrepancy between the exact and approximate values is seen to occur at 50 keV, at which the difference is about 2%. At 200 keV, on the other hand, the linear approximation of the exponential function is seen to be accurate to within 0.2%. It will be shown below that the most probable energy of a photon within a typical burst is about 100 keV. The linear approximation agrees with the exponential at that energy to with 0.5%. It would appear reasonable then to approximate the first exponential appearing in Eqn. (7) by its linear representation, and thereby obtain angular locations which will be "first order," a refinement over the "zero-th order" attainment based on totally ignoring attenuation effects.

Table II displays values of attenuation coefficients of sodium iodide[4] over the energy range of interest, along with values of the second exponential factor appearing in Eqn. (7). It is seen that for a 1.27 cm-thick crystal, this factor is

essentially unity up to about 125 keV. It is important to recognize, however, that the values displayed in the fourth column correspond to normal incidence and thus correspond to minimum values of $(1 - e^{-\mu D/\cos\alpha})$. Alternatively, that column can be looked upon as exhibiting the proximity of this factor to unity. More typically an angle of incidence $\alpha \sim 45°$ might be encountered, thus requiring photons to traverse a greater thickness of the crystal, while increasing their probability of detection. The latter values are tabulated in the fifth column. It should be noted here that if these same considerations regarding the angle of incidence were given to Table I that the exponential factor and its linear approximation would be in agreement to within 0.8%. The burst location discussion presented here will assume validity of the linear approximation of attenuation in the aluminum window and that the crystal will respond to any photon which enters it.

Gamma rays within the 50 - 150 keV then can be expected to give rise to the following approximate forms of Eqn. (7):

$$N_i(E),\theta,\phi) \simeq I_o A(\cos\alpha_i - \mu_A(E)t) \qquad (8)$$

The fact that the attenuation coefficient of sodium iodide no longer appears in this approximation allows the subscript to be dropped from μ_A; hereafter $\mu(E)$ will refer to aluminum.

BURST LOCATION DETERMINATION

Use of Eqn. (8) in determining the angular coordinates of a burst source will now be described. The energy dependence of the results will be emphasized and location formulas including the energy dependent term in Eqn. (8) will be derived.

Consider a burst activiting detectors 1 through 4. (This means that $55° < \theta < 125°$ and $45° < \phi < 135°$. Generalization of the results to other detector combinations will be discussed later.) Using the definition of $\cos\alpha_i = (\vec{I}/I_o)\cdot(-\hat{u}_i)$ along with Eqns. (1) and (3) gives the following expressions for the $\cos\alpha_i$ in terms of θ and ϕ:

$$\begin{aligned}
\cos\alpha_1 &= \frac{1}{\sqrt{3}}(\sin\theta\cos\phi + \sin\theta\sin\phi + \cos\theta) , \\
\cos\alpha_2 &= \frac{1}{\sqrt{3}}(-\sin\theta\cos\phi + \sin\theta\sin\phi - \cos\theta) , \\
\cos\alpha_3 &= \frac{1}{\sqrt{3}}(-\sin\theta\cos\phi + \sin\theta\sin\phi + \cos\theta) , \\
\cos\alpha_4 &= \frac{1}{\sqrt{3}}(-\sin\theta\cos\phi + \sin\theta\sin\phi - \cos\theta) .
\end{aligned} \tag{9}$$

At this point two important identities between the $\cos\alpha_i$ should be noted. It can be immediately seen from inspection of the statements given in Eqn. (9) that

$$\cos\alpha_4 = \cos\alpha_3 + \cos\alpha_2 - \cos\alpha_1 . \tag{10}$$

This relationship simply restates the last connection between the $\hat{u}_i$ noted in Eqn. (2) and indicates the sufficiency for the use of three detectors only. A less obvious but, as will be seen below, very important additional identify which can be easily verified is the following:

$$(\cos\alpha_1 - \cos\alpha_2)^2 = \frac{4}{3} - [(\cos\alpha_2 + \cos\alpha_3)^2 + (\cos\alpha_1 - \cos\alpha_3)^2] \quad .(11)$$

It is reasonable to expect that burst location determinations could be made with increased confidence for the case of the more highly activated detectors. Eqn. (10) will allow those determinations to be made in terms of the three highest detector responses, assumed here to be N_1, N_2, and N_3. The number of photons incident from a given burst, I_oA, appears in each detector statement of the form given in Eqn. (8). This quantity is unknown, however, and Eqn. (11) serves the purpose of allowing it to be determined.

Combining Eqns. (9) and (8) gives the following system:

$$\begin{aligned} N_1 &= \frac{1}{\sqrt{3}} I_o A[\sin\theta\cos\phi + \sin\theta\sin\phi + \cos\theta - \mu(E)t] \\ N_2 &= \frac{1}{\sqrt{3}} I_o A[\sin\theta\cos\phi + \sin\theta\sin\phi - \cos\theta - \mu(E)t] \qquad (12) \\ N_3 &= \frac{1}{\sqrt{3}} I_o A[-\sin\theta\cos\phi + \sin\theta\sin\phi + \cos\theta - \mu(E)t] \end{aligned}$$

The explicit statement for N_4 will be suppressed since Eqn. (10) implies that $N_4 = N_3 + N_2 - N_1$. It is more convenient to express

the angular functions of Eqn. (12) in terms of a "corrected count" expressed as

$$N_i' = N_i + \frac{1}{3} I_o A\mu(E)t \ ; \tag{13}$$

Then

$$N_1' = \frac{1}{\sqrt{3}} I_o A(\sin\theta \cos\phi + \sin\theta \sin\phi + \cos\theta) \ ,$$

$$N_2' = \frac{1}{\sqrt{3}} I_o A(\sin\theta \cos\phi + \sin\theta \sin\phi - \cos\theta) \ , \tag{14}$$

$$N_3' = \frac{1}{\sqrt{3}} I_o A(-\sin\theta \cos\phi + \sin\theta \sin\phi + \cos\theta) \ .$$

Eqns. (14) are easily combined to yield expressions which can be solved for θ and ϕ. It is apparent that

$$N_2' + N_3' = \frac{2}{\sqrt{3}} I_o A \sin\theta \sin\phi \ , \tag{15}$$

and

$$N_1' - N_3' = \frac{2}{\sqrt{3}} I_o A \sin\theta \cos\phi \ . \tag{16}$$

Division of these and use of Eqn. (13) gives

$$\tan\phi = \frac{N_2' + N_3'}{N_1' - N_3'} = \frac{N_2 + N_3}{N_1 - N_3} + \frac{\frac{2}{\sqrt{3}} I_o A\mu(E)t}{N_1 - N_3} \tag{17}$$

The second term on the right of Eqn. (17) will be viewed as a connection to the azimuthal location of the burst, and is due to the finite thickness of the detectors' aluminum window. Its significance will later be discussed in detail.

The expression for $\tan\phi$ given in Eqn. (17) can be used to construct $\sin\phi$; the result is, in terms of the N_i',

$$\sin\phi = \frac{N_2' + N_3'}{(N_1' - N_3')^2 + (N_2' + N_3')^2} . \qquad (18)$$

The statements in Eqn. (14) further give

$$N_1' - N_2' = \frac{2}{\sqrt{3}} I_o A \cos\theta , \qquad (19)$$

and

$$N_2' + N_3' = \frac{2}{\sqrt{3}} I_o A \sin\theta \sin\phi . \qquad (20)$$

Division of these and use of Eqns. (13) and (18) gives

$$\tan\theta = [N_1'^2 + N_2'^2 + N_3'^2 + 2N_3'(N_2 - N_1)]^{1/2} \qquad (21)$$

The expressions for determining θ and ϕ in terms of N_1, N_2, and N_3 are seen to be energy dependent and contain the unknown flux density I_o. The latter quantity can be eliminated from Eqns. (17) and (21) by expressing it in terms of the detector counts. This can be achieved by use of the $\cos\alpha_i$ identity given in Eqn. (11). In terms of the N_i',

$$\left(\frac{N_1'}{I_o A} - \frac{N_2'}{I_o A}\right)^2 = \frac{4}{3} - \left[\left(\frac{N_2'}{I_o A} + \frac{N_3'}{I_o A}\right)^2 + \left(\frac{N_1'}{I_o A} - \frac{N_3'}{I_o A}\right)^2\right] \qquad (22)$$

If the N_i' are expressed according to Eqn. (13) a quadratic in $I_o A$ results which has solution

$$I_oA = \frac{2\mu(E)t(N_2 + N_3)}{\left[\frac{4}{3} - 4(\mu(E)t)^2\right]} +$$

$$\frac{\left\{\left[2\mu(E)t(N_2+N_3)\right]^2+\left[\frac{4}{3} - 4(\mu(E)t)^2\right]\left[(N_1- N_2)^2+(N_1- N_3)^2+(N_2+N_3)^2\right]\right\}^{1/2}}{\left[\frac{4}{3} - 4(\mu(E)t)^2\right]} \quad (23)$$

The negative root has been discarded by the requirement $I_oA > 0$.

Equations (17) and (21), along with (23), are sufficient to determine the angular location of the burst source for photons of energy between 50 keV and, perhaps, 150 keV. The expressions to which these quantities reduce in the limit $t \to 0$ are those which can easily be derived by ignoring attenuation (and thus energy) effects from the outset. The latter expressions, as previously mentioned, can be thought of as "zero-th order expressions" and will hereafter be superscripted "(o)". Explicitly,

$$\tan\phi^{(o)} = \frac{N_2 + N_3}{N_1 - N_3}, \quad (24)$$

$$\tan\theta^{(o)} = \frac{\left[N_1^2 + N_2^2 + 2N_3^2 + 2N_3(N_2 - N_1)\right]^{1/2}}{N_1 - N_2} \quad (25)$$

and

$$(I_oA)^{(o)} = \frac{\sqrt{3}}{2}\left[(N_1 - N_2)^2 + (N_1 - N_3)^2 + (N_2 + N_3)^2\right]^{1/2}. \quad (26)$$

That neither Eqn. (24) nor (25) contains the flux density explicitly means that Eqn. (26) need not be evaluated for locations in this order.

The effect of the aluminum window on burst location determination is seen, by comparing Eqns. (17) with (24) and (21) with (25), to give rise to an abberation. The role of the energy dependence in this abberation will now be examined. Computations of the source location and flux density must be made in terms of detector counts. The energy influence on these quantities can perhaps best be illustrated by choosing reasonable values of what might typify data registered by the three detectors. For this purpose let $N_1 = 3$, $N_3 = 2$, and $N_3 = 1$. (These numbers have, of course, been scaled down by $\sim 10^3$, which is permissible since only the relative counts really matter.) These values give, with t = 0.2 cm and Eqns. (23), (17), and (21) the results displayed in Table III. The deviations, $\delta\phi = \phi - \phi^{(o)}$ and $\delta\theta = \theta - \theta^{(o)}$, are seen to diminish with increasing energy. This result is what would be expected, as the attenuation would be reduced for the more energetic photons. It would appear, however, that in no case displayed there is the deviation negligably small.

Although not small with respect to burst location determinations $\delta\phi$ and $\delta\theta$ are small in the sense that their tangents can be set equal to these angles (in radians) themselves; e.g., $\tan\delta\phi \approx \delta\phi$. These approximations are known to hold for angles considerably larger than those displayed in Table III and allow general deviation formulas to be derived.

According to Eqn. (17)

$$\tan\phi - \tan\phi^{(o)} = \frac{\frac{2}{\sqrt{3}} I_o A\phi(E)t}{N_1 - N_3} .$$

Setting $\phi = \phi^{(o)} + \delta\phi$, using the addition formula to express $\tan(\phi^{(o)} + \delta\phi)$, with $\tan\delta\phi \approx \delta\phi$ gives

$$\frac{\tan\phi^{(o)} + \delta\phi}{1-\delta\phi\,\tan\phi^{(o)}} - \tan\phi^{(o)} = \frac{\frac{2}{\sqrt{3}} I_o A\mu(E)t}{N_1 - N_3} .$$

Solving for $\delta\phi$ and expressing $\tan\phi^{(o)}$ according to Eqn. (24) gives the result

$$\delta\phi = \frac{\frac{2}{\sqrt{3}} I_o A\mu(E)t(N_1-N_2)}{(N_1-N_3)^2 + (N_2+N_3)^2 + \frac{2}{\sqrt{3}} I_o A\mu(E)t(N_2+N_3)} . \qquad (27)$$

As might be anticipated from Eqn. (21) the corresponding calculation of $\delta\theta$ is more involved. The fact that $\tan\theta$ is expressed in terms of a square root necessitates solving a quadratic equation in $\delta\theta$. The somewhat laborous details of the calculation will be omitted here in favor of getting on with the result:

$$\delta\theta_{\pm} = \frac{-\tan\theta^{(o)}[1+C+\tan^2\theta^{(o)}]}{[1 - C\tan^2\theta^{(o)} - \tan^4\theta^{(o)}]} \qquad (28)$$

$$\pm \frac{\{\tan^2\theta^{(o)}[1+C+\tan^2\theta^{(o)}]^2 + C[1-C\tan^2\theta^{(o)} - \tan^4\theta^{(o)}]\}^{1/2}}{[1 - C\tan^2\theta^{(o)} - \tan^4\theta^{(o)}]}$$

where $\tan\theta^{(o)}$ is given by Eqn. (25) and

$$C = \frac{\frac{4}{\sqrt{3}} I_o A\mu(E)t(N_2+N_3 + \frac{1}{\sqrt{3}} I_o A\mu(E)t)}{(N_1-N_2)^2} . \qquad (29)$$

The choice of sign is made according to the requirement that $\delta\theta_{\pm} \to 0$ as $t \to 0$ (i.e., as $C \to 0$). This means that if $\tan\theta^{(o)} > 0$, choose $\delta\theta_{+}$; if $\tan\theta^{(o)} < 0$, choose $\delta\theta_{-}$. It might appear that $\delta\theta$ would become infinite for that value of $\theta^{(o)}$ which causes the denominator to vanish. It must be kept in mind that the above was derived under the premise of the activation of detectors 1 through 4. This means that $55^0 \lesssim \theta \lesssim 125^0$; it is easily shown that the value of $\theta^{(o)}$ which would cause the denominator of Eqn. (28) to vanish is not within this range.

The fact that the deviation formulas are energy dependent makes their expressions, Eqns. (27) and (28), somewhat difficult to interpret. (It should be kept in mind that the N_i appearing in those expressions are themselves effected by gamma ray energy: the fact that μ decreases with increasing energy means, according to the relations given in Eqn. (12), that the N_i will correspondingly increase and thereby additionally influence $\delta\phi$ and $\delta\theta$.) The significance of these formulas might best be appreciated by expressing the deviations in terms of the most probable energy of a photon in a burst over the 50 - 150 keV range.

Burst spectra so far obtained appear to obey the following empirical relation[5]:

$$\frac{dn}{dE} \propto \frac{1}{E^{1.4}} .$$

The most probable energy, $\langle E \rangle$, is then calculated as

$$\langle E \rangle = \frac{\int n(E)EdE}{\int n(E)dE} , \qquad (30)$$

integrated over the afore-mentioned limits. The result for the above power law gives $\langle E \rangle$ = 96.4 keV.

The deviations given by Eqns. (27) and (28) can now be assessed at this value of energy for various detector counts. Table IV displays a variety of detector response examples along with the corresponding deviations at 96.4 keV. (The value of μ used here was 0.513 cm^{-1}.) The column headed "$(\delta\theta_{\pm})$" has been included to indicate the choice of sign used in Eqn. (28). The zero values in $\delta\phi$ and $\delta\theta$ result from the equality of N_1 and N_3, and N_1 and N_2, respectively.

DISCUSSION AND CONCLUSIONS

Burst location determinations based on detector responses have been discussed in a way that includes gamma ray energies. Equations (17) and (21), along with (23) can be used for energies in the approximate range 50 - 150 keV. Although those expressions were developed under the assumption of a burst activating detectors 1 through 4, so that at least two of these have $N_i > 0$, it is a straight-forward matter to generate the appropriate expressions in the event of activation of some other detector combination. The unit vector relationships given in Eqn. (2) indicate, e.g., that $N_7 = -N_4$ and $N_8 = -N_3$. Thus, if a burst activated detectors 1, 2, 7, and 8 it would only be necessary to replace N_3 in the expressions given by $-N_8$. N_2 need

not appear in the final expression, as was the case with N_4 in the situation discussed, since $N_2 = N_1 + N_8 - N_7$. The deviation formulas can be similarly altered.

The examples of deviations associated with the detector responses considered in Table IV assumed a particular power-law energy spectrum of the burst in order to compute the most probable energy, <E>. This quantity can easily be calculated from Eqn. (30) for any burst spectrum. If, for example, the spectrum[6] $dn/dE \propto \exp(-E/E_o)$, where E_o = 150 keV, were used then <E> = 94.5 keV. This value is only slightly different from that used in generating Table IV.

It has been demonstrated that energy considerations connected with the role of the passive absorber shielding each detector are significant if locations are to be determined to within a few degrees. A major objective of the BATSE is to make those determinations to within less than 1°. It would therefore seem necessary to incorporate the effects discussed in the present work into the overall scheme of location determinations.

The difficulties involved in obtaining angular (θ,ϕ) solutions from a set of statements of the form given by Eqn. (7) are apparent. The efforts of the present study were restricted to obtaining first order corrections to the locations given by Eqns. (24) and (25). It has been found possible to obtain the second order correction corresponding to the retention of an additional term in the expansion of the aluminum exponential expansion. The details of that calculation have not yet been fully explored, but can and should be done.

The need to impose the upper limit on the energy range as discussed here to 150 keV resulted from the detector efficiency decreasing too rapidly above this energy (as well as somewhat below it). Further investigation is clearly necessary so that the upper limit can approach the desired 200 keV value. It is not entirely clear at this point that those calculations can be performed analytically.

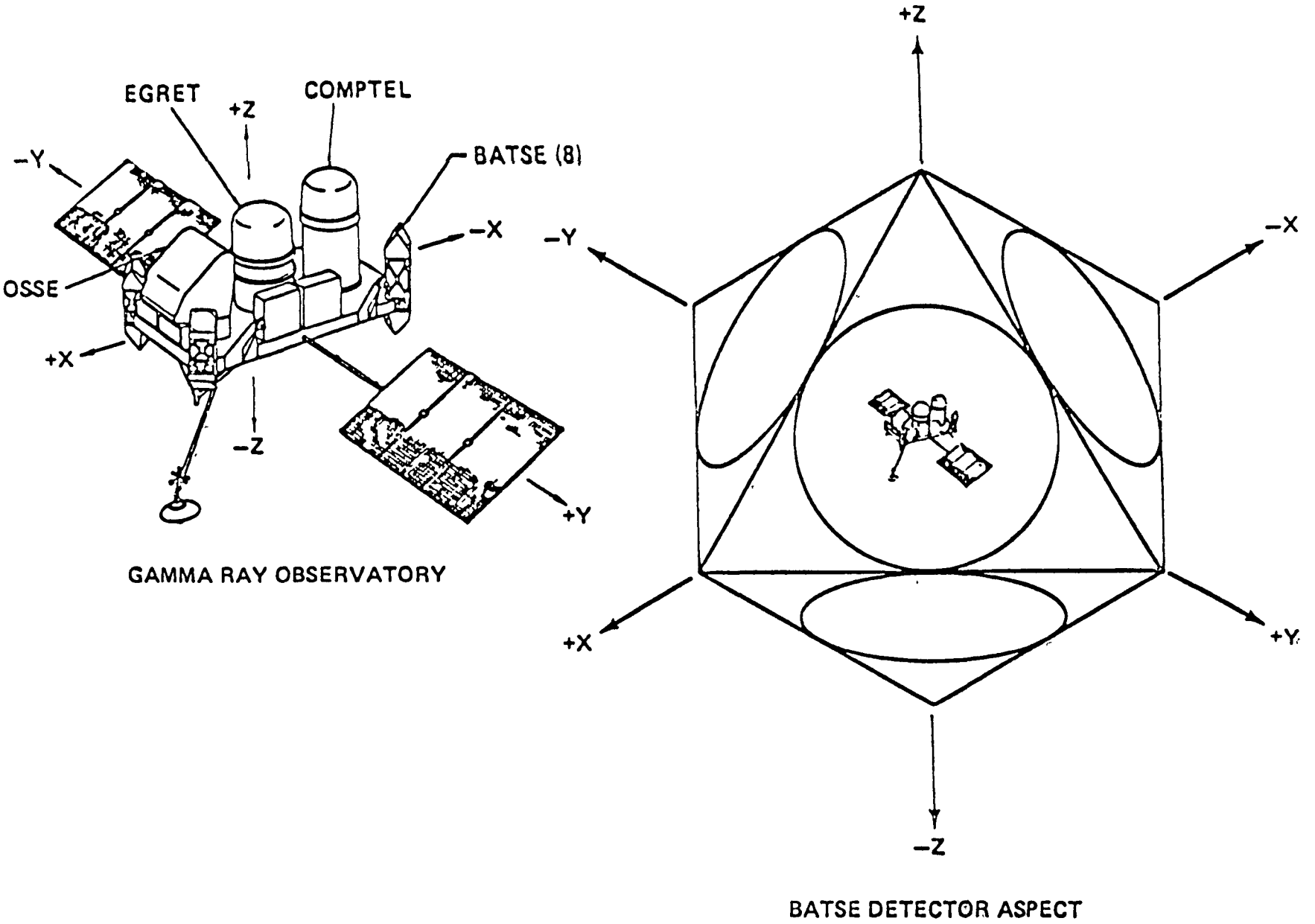

Figure 1. Gamma Ray Observatory Configuration; BATSE Octohedral Geometry

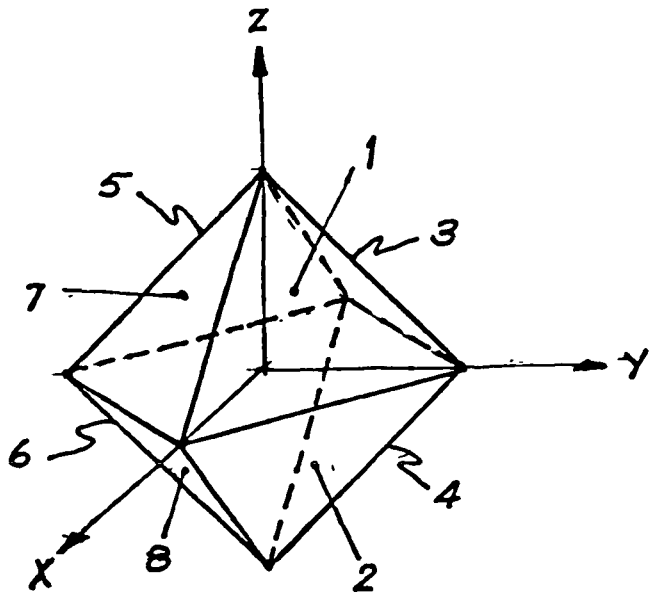

Figure 2. Plane Identification Scheme in the Octohedral Geometry

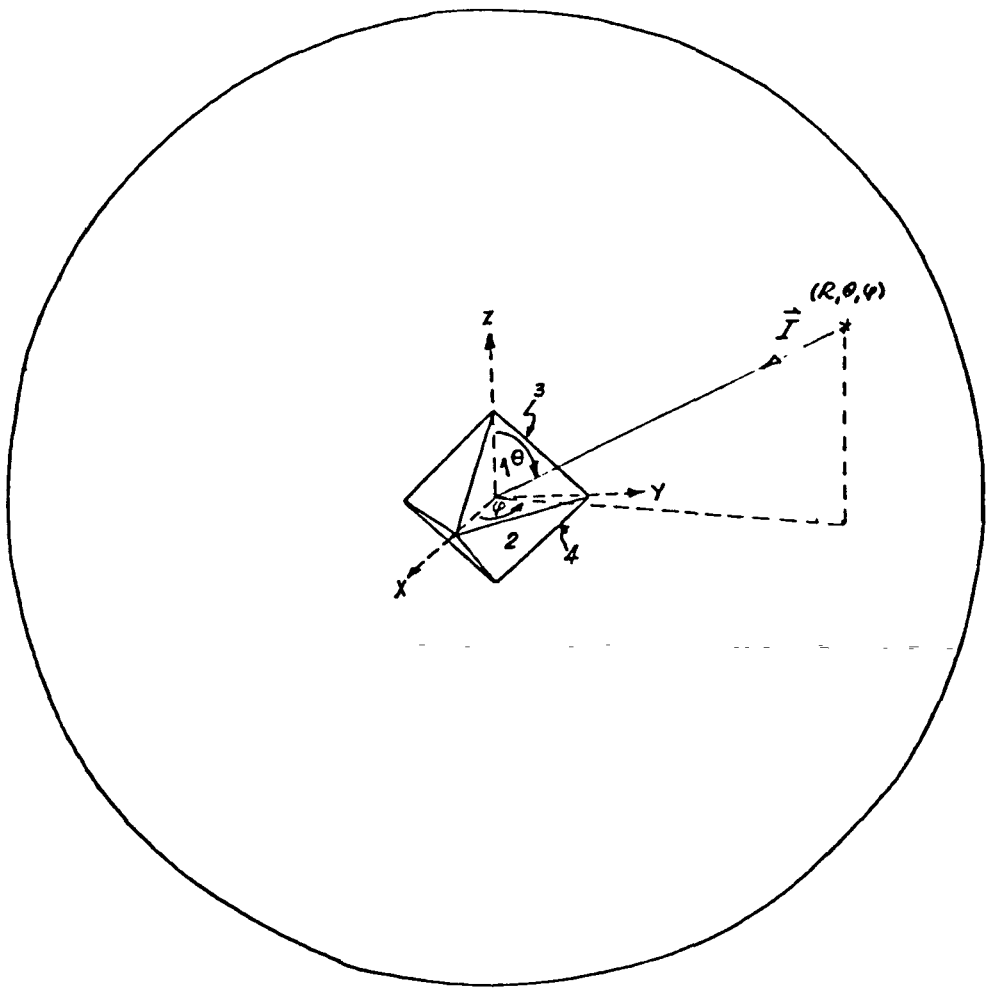

Figure 3. Burst Propagation Toward the BATSE Geometry

TABLE I

Attenuation Coefficients for Aluminum and Evaluation of Their Influence

E(keV)	$\mu(cm^{-1})$	$e^{-\mu t}$	$1-\mu t$
50	0.972	0.823	0.806
75	0.621	0.883	0.876
100	0.473	0.910	0.905
125	0.405	0.922	0.919
150	0.378	0.927	0.924
175	0.351	0.932	0.930
200	0.324	0.937	0.935

TABLE II

Attenuation Coefficients for Sodium Iodide and Evaluation of Their Influence

E(keV)	$\mu(cm^{-1})$	$e^{-\mu D}$	$(1-e^{-\mu D})$	$(1-e^{-\mu D/\cos 45^0})$
50	36.70	5.7×10^{-21}	~1	~1
75	12.85	2.6×10^{-6}	~1	~1
100	6.97	1.4×10^{-4}	~1	~1
125	3.67	9.8×10^{-3}	0.99	~1
150	2.20	6.1×10^{-2}	0.94	0.98
175	1.47	0.155	0.85	0.93
200	1.28	0.278	0.72	0.90

TABLE III

Computed Angular Deviations of Source as a Function of Energy and Fixed N_1, N_2, N_3

E(keV)	I_oA	ϕ	θ	$\phi^{(o)}$	$\theta^{(o)}$	$\delta\phi$	$\delta\theta$
50	4.57	63.58°	77.44°	56.31°	74.50°	7.27°	2.94°
75	3.96	60.73°	76.26°	56.31°	74.50°	4.42°	1.76°
100	3.75	59.61°	75.80°	56.31°	74.50°	3.30°	1.30°
125	3.67	59.11°	75.60°	56.31°	74.50°	2.80°	1.10°
150	3.64	58.92°	75.53°	56.31°	74.50°	2.61°	1.03°

TABLE IV

Computed Angular Deviations of Source for <E> and Various N_1, N_2, $N_3(x10^n)$

N_1	N_2	N_3	I_oA	$\delta\phi$	$\delta\theta$	$(\delta\theta_+)$
3	2	1	3.80	+3.59°	+1.42°	(+)
1	3	2	5.68	-1.31°	-2.27°	(-)
2	1	3	4.42	-1.57°	+1.45°	(+)
2	2	3	5.35	-1.31°	0°	
3	2	2	4.42	+1.57°	+1.45°	(+)
2	3	2	5.35	0°	-1.25°	(-)

REFERENCES

1. G. J. Fishman, et al.: BATSE/GRO Observational Capabilities, Space Science Laboratory Preprint Series No. 84-103.

2. S. S. Holt in Introduction to Experimental Techniques of High-Energy Astrophysics, H. Ogleman and J. R. Wayland, ed., NASA Office of Technology Utilization, 1970.

3. J. H. Hubbell: Photon Cross Sections, Attenuation Coefficients, and Energy Absorption Coefficients from 10 keV to 100 GeV, NBS-29, National Bureau of Standards, 1969.

4. R. D. Evans: The Atomic Nucleus, McGraw-Hill Book Company, New York, p. 717, 1955.

5. G. J. Fishman, private communication.

6. E. C. Chupp: Gamma Ray Astronomy, D. Reidel Publishing Company, Dordrecht-Holland/Boston, p. 196, 1976.

☆U S GOVERNMENT PRINTING OFFICE 1986–631-058/20081